Implementation of Empirical Dispersion Corrections to Density Functional Theory for Periodic Systems

Werner Reckien,[a] Florian Janetzko,[b] Michael F. Peintinger,[a] and Thomas Bredow*[a]

A recently developed empirical dispersion correction (Grimme et al., J. Chem. Phys. 2010, 132, 154104) to standard density functional theory (DFT-D3) is implemented in the plane-wave program package VASP. The DFT-D3 implementation is compared with an implementation of the earlier DFT-D2 version (Grimme, J. Comput. Chem. 2004, 25, 1463; Grimme, J. Comput. Chem. 2006, 27, 1787). Summation of empirical pair potential terms is performed over all atom pairs in the reference cell and over atoms in shells of neighboring cells until convergence of the dispersion energy is obtained. For DFT-D3, the definition of coordination numbers has to be modified with respect to the molecular version to ensure convergence. The effect of three-center terms as implemented in the original molecular DFT-D3 version is investigated. The empirical parameters are taken from the original DFT-D3 version where they had been optimized for a reference set of small molecules. As the coordination numbers of atoms in bulk and surfaces are much larger than in the reference compounds, this effect has to be discussed. The results of test calculations for bulk properties of metals, metal oxides, benzene, and graphite indicate that the original parameters are also suitable for solid-state systems. In particular, the interlayer distance in bulk graphite and lattice constants of molecular crystals is considerably improved over standard functionals. With the molecular standard parameters (Grimme et al., J. Chem. Phys. 2010, 132, 154104; Grimme, J. Comput. Chem. 2006, 27, 1787) a slight overbinding is observed for ionic oxides where dispersion should not contribute to the bond. For simple adsorbate systems, such as Xe atoms and benzene on Ag(111), the DFT-D implementations reproduce experimental results with a similar accuracy as more sophisticated approaches based on perturbation theory (Rohlfing and Bredow, Phys. Rev. Lett. 2008, 101, 266106). © 2012 Wiley Periodicals, Inc.

DOI: 10.1002/jcc.23037

Introduction

Density functional theory (DFT) is currently the most widely used method in quantum-chemical molecular and solid-state calculations.[1] In solid-state chemistry and physics the local density approximation is still popular, but is now superseded by the generalized gradient approximation (GGA) and meta-GGA functionals.[2] It is well known that standard local and semilocal DFT methods fail to describe dispersion effects that are of nonlocal nature. Consequently, DFT methods are often inaccurate for calculations of molecular crystals, adsorption on surfaces, and other systems in which dispersion forces play a significant role for the structure and energetics.

In the last years much effort has been spent to remedy this situation. Specially parameterized hybrid meta-exchange functionals have been developed and tested for noncovalent interactions.[3] Approximate nonlocal functionals have been designed particularly for dispersion interactions (vdW-DFT).[4–6] Combination of exact Hartree-Fock exchange with correlation energy derived from the adiabatic connection fluctuation-dissipation theorem has been suggested.[7] A similar idea was proposed independently by Rohlfing and Bredow.[8] The latter methods are based on first principles and computationally demanding. An empirical, but much more efficient approach is an *a posteriori* correction of the total Kohn-Sham energy by effective interatomic potentials. Such simple schemes have been proposed some time ago, see for example, Ref. [9]. A recent review discussing advantages and drawbacks of the various approaches to dispersion in solid-state quantum-chemistry can be found in Ref. [10].

For molecular systems, Grimme et al.[11–14] proposed several versions of a damped empirical correction term called DFT-D. One major difference between these approaches is the way to calculate the empirical dispersion (C_6) coefficients. The DFT-D2 correction[13] and the original parameterization[12] use an empirically derived interpolation formula, whereas the D3 correction is a novel approach based on an *ab initio* calculation of the C_6 (and, additionally, C_8) coefficients.[11] The most recent DFT-D3BJ scheme[14] differs from DFT-D3 essentially only in the weighting function. In all cases, the dispersion energy is calculated separately from the DFT energy and does not depend on the wavefunction. It does therefore not take into account polarization effects and is solely a function of the atomic positions and of the atom type. One advantage of the D*n* correction schemes is their computational efficiency and careful parameterization. For molecules DFT-D3 provides

[a] *W. Reckien, M. F. Peintinger, T. Bredow*
Mulliken Center for Theoretical Chemistry, Institut für Physikalische und Theoretische Chemie, Universität Bonn, Beringstr. 4, D-53115 Bonn, Germany
E-mail: bredow@thch.uni-bonn.de

[b] *F. Janetzko*
Jülich Supercomputing Centre, Institute for Advanced Simulation, Forschungszentrum Jülich GmbH, 52425 Jülich, Germany

Contract/grant sponsor: Collaborative Research Center SFB 624, Deutsche Forschungsgemeinschaft.

results close to the coupled cluster singles doubles with perturbative triples (CCSD(T)) values at the cost of GGA-DFT calculations.[11] However, as the DFT-D3 method is parameterized for molecular benchmark sets it is not self-evident that its applicability can be transferred to periodic systems. This is basically due to the hybridization-dependent C_6 coefficients that are based on the coordination number (*CN*). The *CN*-dependent C_6 coefficients are extrapolated from a reference set that contains only small molecules and atoms. A systematic investigation of the transferability of these approaches to solids and surfaces with much higher CNs has been the subject of recent studies. For Mg, Na,[15] and Ti (Möllmann et al., in preparation) it was found that the C_6 coefficients decrease with increasing *CN* due to the smaller dynamic polarizability. This is in agreement to a previous work where it was found that the Mg C_6 parameter for the D2 correction in MgO has to be reduced by one magnitude compared with the value for the Mg atom.[16] The extended D3 parameter set results in a slight improvement of adsorption energies for acetylene on NaCl and CO on MgO,[15] whereas the changes in energy and geometry of bulk MgO, NaCl, and TiO_2 are small. The C_6 parameters for coinage metals Cu, Ag, Au are already converged with the small CNs contained in the standard reference set (Grimme, private communication). For these reasons we did not consider reoptimization of the C_6 parameters in this study. All calculations were performed with the standard parameter set.[11]

In recent years, the D2 correction was frequently used for periodic systems,[17–26] whereas to the best of our knowledge the D3 correction has been used only as *a posteriori* correction to the total energy for the glycine adsorption on Cr_2O_3,[27] and in our recent study[15] so far.

In the following, we present our implementation of the D3 correction into the plane-wave program package VASP[28] which is widely used in quantum solid-state chemistry. We also briefly discuss our implementation of the D2 correction as it differs from the standard implementation in VASP 5.2.11[19] in several details that will be described below.

We begin this article with a brief review of the DFT-D2 and DFT-D3 approaches for molecules and describe their extension to periodic systems. Details of our implementation in the VASP package are given in the following section. Then we apply the D2 and D3 corrections to selected solids and surfaces. Results are presented for systems where standard DFT fails due to insufficient description of dispersion interaction but also for systems which are correctly described by standard DFT. For the latter systems, it is important to investigate if an empirical dispersion correction causes a deterioration of the results due to an overbinding.

Theory

Empirical dispersion terms

The total energy is calculated as the sum of the self-consistent Kohn-Sham-DFT (KS-DFT) energy E_{DFT} and the dispersion energy E_{D2}[12,13] and E_{D3}, respectively.[11,14]

$$E_{DFT+D2} = E_{DFT} + E_{D2}$$

$$E_{DFT+D3} = E_{DFT} + E_{D3}$$

E_{D2} and E_{D3} are empirical correction terms calculated as sums over atom pairs (A, B).

The D2 correction describes the dispersion correction according to:

$$E_{D2} = -s_6 \sum_{B>A}^{N} \frac{C_6^{AB}}{R_{AB}^6} f_{dmp}(R_{AB}) \quad (1)$$

Here, N denotes the number of atoms in the molecule, s_6 is a functional-dependent scaling factor, C_6^{AB} are the dispersion coefficients, R_{AB} is the distance between the two atoms A and B, and $f_{dmp}(R_{AB})$ is a damping function which screens out the dispersion interactions at short distances.

$$f_{dmp}(R_{AB}) = \left[1 + e^{-d\left(\frac{R_{AB}}{R_{vdw}} - 1\right)}\right]^{-1}$$

R_{vdw} is the sum of the atomic van-der-Waals radii and d is an empirical scaling parameter.[13] The composed dispersion coefficients C_6^{AB} are calculated as the geometric mean of the atomic coefficients C_6^{A}:

$$C_6^{AB} = \sqrt{C_6^A \, C_6^B}$$

Within the framework of the D3 correction the dispersion energy is the sum of two-body ($E^{(2)}$) and three-body ($E^{(3)}$) terms:

$$E_{D3} = E^{(2)} + E^{(3)}$$

With this ansatz $E_{D3} = E^{(2)}$ is given by:

$$E^{(2)} = \sum_{B>A}^{N} \sum_{n=6,8} s_n \frac{C_n^{AB}}{R_{AB}^n} f_{d,n}(R_{AB}) \quad (2)$$

Here, C_n^{AB} is the n-th-order dispersion coefficient ($n = 6,8$) for atom pair (AB). s_8 is an empirical global functional-dependent scaling factor, s_6 is equal to 1 for all GGA and hybrid functionals. R_{AB} is the distance between atoms A and B. The damping function

$$f_{d,n}(R_{AB}) = \frac{1}{1 + 6\left(\frac{R_{AB}}{s_{r,n} \cdot R_0^{AB}}\right)^{-\alpha_n}}$$

determines the range of the dispersion correction. To allow variation of dispersion coefficients with the chemical environment the C_n^{AB} coefficients depend on the fractional *CN*. *CN* for atom A is obtained in the following way:

$$CN^A = \sum_{B \neq A} \left[1 + e^{-k_1\left(k_2 \cdot \frac{R_{A,cov} + R_{B,cov}}{R_{AB}} - 1\right)}\right]^{-1} \quad (3)$$

$R_{A,cov}$ and $R_{B,cov}$ are scaled single-bond radii, and $k_1 = 16$ and $k_2 = \frac{4}{3}$ are scaling parameters. The CN dependent dispersion coefficients $C_6^{AB}(CN^A,CN^B)$ are obtained by a two-dimensional interpolation scheme from the $C_{6,ref}^{AB}(CN^A,CN^B)$ coefficients of a reference set which consists of 254 atoms and small molecules:

$$C_6^{AB}(CN^A, CN^B) = \frac{\sum_i^{N_A}\sum_j^{N_B} C_{6,ref}^{AB}(CN_i^A, CN_j^B)\cdot L_{ij}}{\sum_i^{N_A}\sum_j^{N_B} L_{ij}} \quad (4)$$

$$L_{ij} = e^{-4\left(\left(CN^A-CN_i^A\right)^2+\left(CN^B-CN_j^B\right)^2\right)} \quad (5)$$

Here, N_A and N_B are the numbers of the reference molecules for atoms A and B, CN_i^A and CN_j^B are their fractional CNs within the reference systems i and j and $C_{6,ref}^{AB}(CN_i^A,(CN_j^B)$ is the corresponding dispersion coefficient. The $C_8^{AB}(CN^A,CN^B)$ coefficients are calculated from the $C_6^{AB}(CN^A,CN^B)$ coefficients.[11]

To take into account nonadditive effects of dispersion interaction three-body terms have been introduced:

$$E^{ABC} = \frac{C_9^{ABC}(3\cos(\theta_a)\cos(\theta_b)\cos(\theta_c)+1)}{r_{AB}r_{BC}r_{CA}}$$

Hereby, θ_a, θ_b and θ_c are the angles of the triangle which is formed by atoms A, B, and C. The C_9^{ABC} coefficients are approximated by the geometric mean of the C_6^{ij}-coefficients:

$$C_9^{ABC} = -\sqrt{C_6^{AB}C_6^{AC}C_6^{BC}}$$

The $E^{(3)}$ contribution to E_{D3} is calculated by multiplying E^{ABC} with the damping function $f_{d,(3)}(\bar{r}_{ABC})$ and summing over all atom triples *ABC*:

$$E^{(3)} = \sum_{ABC} f_{d,(3)}(\bar{r}_{ABC})E^{ABC}$$

For small molecules the two-center terms dominate the dispersion correction so that the $E^{(3)}$ contribution is usually neglected.[15] Their effect on properties of extended systems is discussed in the next section.

Extension to periodic systems

To extend the ansatz of eq. (1) and (2) to periodic systems the dispersion energy correction is calculated per reference cell and includes the two-center terms of (i) the atoms in the reference cell with themselves and (ii) the reference cell with neighboring shells of cells. The resulting term for the D2 correction is:

$$E_{D2}^{cell} = -\frac{s_6}{2}\sum_A^N \sum_{\mathbf{T}=-\mathbf{T}_m}^{\mathbf{T}_m} {}' \sum_B^N \frac{C_6^{AB}}{R_{ABT}^6} f_{damp}(R_{ABT}) \quad (6)$$

and for the D3 correction:

$$E_{D3}^{cell} = -\frac{1}{2}\sum_A^N \sum_{\mathbf{T}=-\mathbf{T}_m}^{\mathbf{T}_m} {}' \sum_B^N \sum_{n=6,8} s_n \frac{C_n^{AB}}{R_{ABT}^n} f_{d,n}(R_{ABT}) \quad (7)$$

Here, $\mathbf{T} = t_a\mathbf{a} + t_b\mathbf{b} + t_c\mathbf{c}$ denotes the distance vector of the neighboring cell T from the reference cell, **a**,**b** and **c** are the lattice vectors and R_{ABT} is the distance between atom A in the reference cell and atom B in the cell T. The primed sum over B indicates that the case $A = B$ is omitted for $\mathbf{T} = \mathbf{0}$. The factor 1/2 is introduced to avoid the double counting of interactions.

Since the two-center terms rapidly decrease with $1/R^6$ or $1/R^8$, only shells up to a predefined threshold $\mathbf{T}_m = t_a^{max}\mathbf{a} + t_b^{max}\mathbf{b} + t_c^{max}\mathbf{c}$ are included. For simplicity, we used in general $t_a^{max} = t_b^{max} = t_c^{max} = t^{max}$ for bulk systems and $t_a^{max} = t_b^{max} = t^{max}$ and $t_c = 1$ for surfaces. $\mathbf{T}_m$ has to be determined for each system by adding successively shells of neighboring cells until the dispersion energy per cell is converged within a given threshold, here 1 kJ/mol. At this point, our ansatz differs from the current implementation of the D2 correction within the VASP code. We use a shell-wise summation over a predefined number of unit cells surrounding the central reference cell instead of a cutoff radius.

As the summation in eq. (7) involves atoms $B_{\mathbf{T}}$ of neighboring cells **T** for which no CN^{B_T} are calculated [required for the calculation of $C_n^{AB\mathbf{T}}$ in eq. (5)], we applied periodic boundary conditions to the CNs:

$$CN^{B_T} = CN^{B_0}$$

Here, **0** denotes the reference cell.

The three-body dispersion correction $E^{(3)}$(cell) is:

$$E^{(3)}(\text{cell}) = -k\sum_A^N \sum_{\mathbf{T}=-\mathbf{T}_m}^{\mathbf{T}_m} \sum_B^N {}' \sum_{\mathbf{T}'=-\mathbf{T}_m}^{\mathbf{T}_m} \sum_C^N {}'' f_{d,(3)}(\bar{r}_{AB_TC_{T'}})E^{AB_TC_{T'}} \quad (8)$$

Here, the primed sum over B indicates that the case $A = B$ is omitted for $\mathbf{T} = \mathbf{0}$, the double primed sum over C indicates that the case B = C is omitted for $\mathbf{T} = \mathbf{T}'$ and A = C is omitted for $\mathbf{T}' = \mathbf{0}$. To avoid multiple counting of the three-body terms the factor k is set to $k = \frac{1}{3}$ if atoms A,B,C are within the reference cell and to $k = \frac{1}{2}$ in all other cases.

Implementation

The dispersion corrections to DFT for periodic systems according to eq. (6), (7), and (8) were implemented in the plane-wave program package VASP.[28] Depending on the chosen density functional E_{D2}^{cell} or E_{D3}^{cell} is added to the standard KS-DFT energy calculated by VASP. To carry out structure optimizations analytic gradients of the dispersion energy with respect to the atomic positions at fixed lattice vectors were implemented. When the three-body terms E^{ABC} are calculated we added the numerical gradient of the three-body-dispersion interaction to the analytical gradient.

A further difference to the original VASP code is that in our present implementation of the D2 correction the atoms of the reference cell can be divided into fragments. This allows a better control over the dispersion interactions. While the dispersion interactions between a fragment and all other fragments in the reference cell and in the neighboring cells are always calculated, one can switch off the dispersion interactions within a fragment

and its translated images either completely or along selected lattice vectors. This procedure may be useful in cases where molecules physisorb on surfaces as it is possible to calculate only the dispersion interaction between the adsorbate (fragment 1) and the surface (fragment 2). We have used this procedure previously for the study of formamide clusters on the Ag(111) surface[29] as PBE-D2 results in an overbinding between the adsorbed hydrogen bonded formamide clusters. We did not implement the fragmentation for the D3 correction.

In periodic DFT-D3 calculations, it is important that not only the dispersion energy per supercell but also the fractional CN must be converged. For the calculation of the CN_{cell} for atoms within the reference cell the summation of the molecular ansatz [eq. (3)] was modified.

$$CN^{A}_{cell} = \sum_{\mathbf{T}=-\mathbf{T}_m}^{\mathbf{T}_m} \sum_{B}^{N} {}' \left[1 + e^{-k_1 \left(k_2 \cdot \frac{R_{A,cov}+R_{B,cov}}{R_{AB}} - 1 \right)} \right]^{-1} \quad (9)$$

Again, the prime indicates that $A = B$ is omitted for $\mathbf{T} = \mathbf{0}$. However, we noticed that CN_{cell} calculated with eq. (9) does not converge with increasing t^{max}, see Figure 1. In most cases, this did not affect the results as the fractional CN^{A}_{cell} in periodical calculations are usually larger than the largest CN^{A}_{i} value of the corresponding reference set, and $C_6^{AB}(CN^A,CN^B)$ did not change with CN_{cell}. The problem is, however, more delicate if CN^{A}_{cell} is in between two CNs of the reference set for atom A. In this case, the $C_6^{AB}(CN^A,CN^B)$ values decrease with increasing t^{max} since the t^{max}-parameters of all reference systems decrease with increasing CN_i, see Ref. [11] for further details.

One example is graphite. The carbon reference set given in Ref. [11] contains (in addition to three other systems with $CN_i < 2$) ethene (C_2H_4) with $CN_4 = 2.99870$ and $C^{CC}_{6,ref}(CN^C_4,CN^C_4) = 25.7809$ a.u. and ethane (C_2H_6) with $CN = 3.98440$ and $C^{CC}_{6,ref}(CN^C_5,CN^C_5) = 18.2067$ a.u. E^{cell}_{D3} seems to be converged for $t^{max} = 8$, see Figure 2. The calculated parameters for carbon

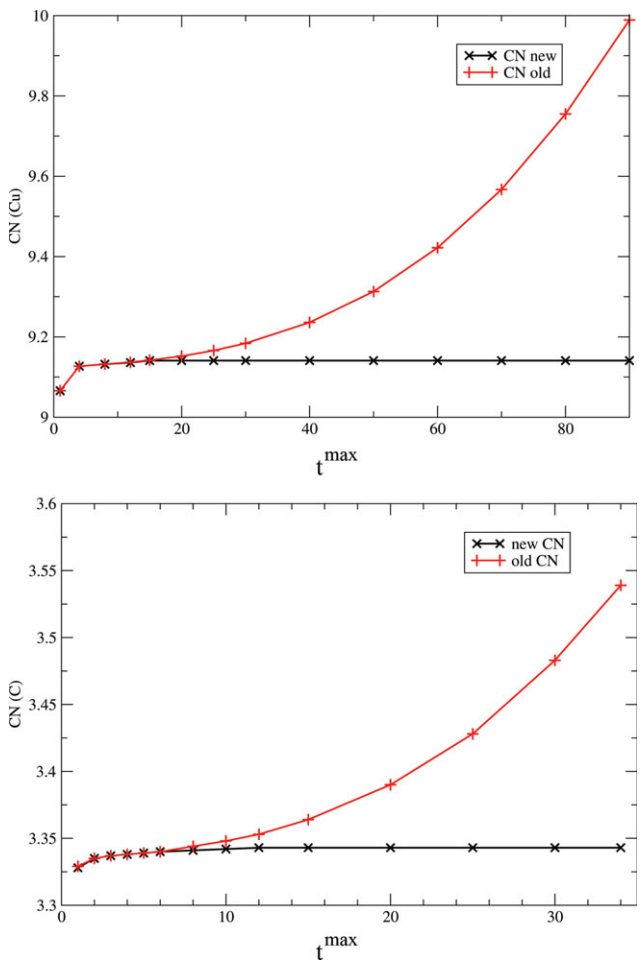

Figure 1. Fractional CN_{cell} calculated according to eq. (3; CN old) and eq. (11; CN new) is plotted against t^{max}. Upper panel: Cu bulk, lower panel: graphite [Color figure can be viewed in the online issue, which is available at wileyonlinelibrary.com.]

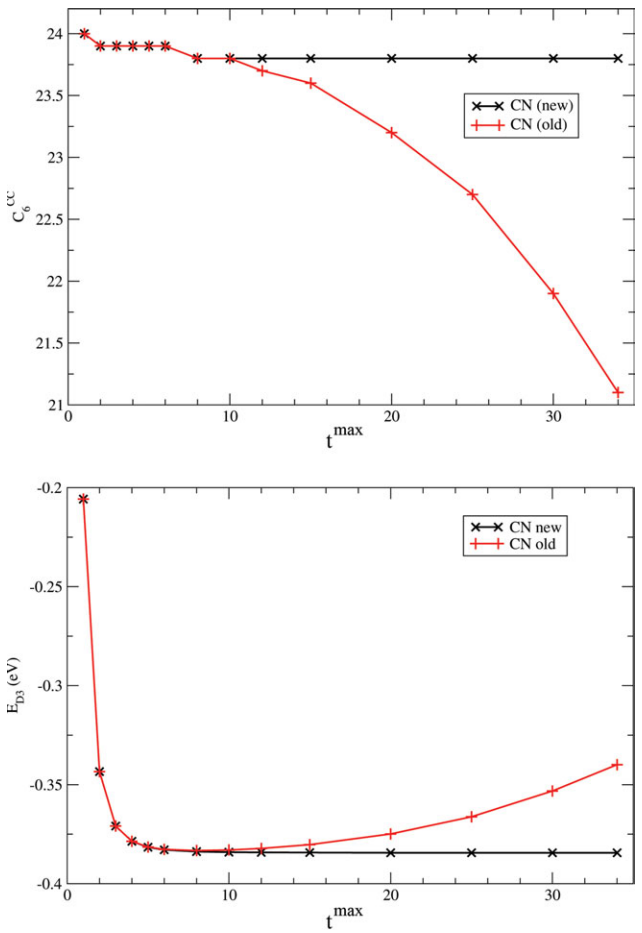

Figure 2. Graphite: Convergence behavior of C_6 and E^{cell}_{D3} with increasing t^{max} [CN according to eq. (3)] [Color figure can be viewed in the online issue, which is available at wileyonlinelibrary.com.]

are $CN = 3.344$ and $C_6^{CC} = 23.8$ a.u. A further increase of t^{max}, however, leads to an increase of CN (e.g., $CN = 3.483$ for $t^{max} = 30$) and in turn to a decrease of the C_6-parameter and E^{cell}_{D3} ($C_6^{CC} = 21.9$ a.u. for $t^{max} = 30$), see Figures 1 and 2. Consequently the dispersion interaction between the graphite layers is reduced and the optimized lattice parameter c is increased. As example, we obtain $c = 6.96$ Å for $t^{max} = 8$, and $c = 7.03$ Å for $t^{max} = 30$ (Fig. 2).

To correct this numerical instability we slightly modified the calculation of the fractional CNs by scaling with a damping function $CN_{\mathrm{damp}}(R_{\mathrm{AB}})$:

$$CN_{\mathrm{damp}}(R_{\mathrm{AB}}) = \frac{1}{2}\mathrm{erfc}\left(R_{\mathrm{AB}} - 15 \cdot k_2 \cdot \left(R_{\mathrm{A,cov}} + R_{\mathrm{B,cov}}\right)\right) \quad (10)$$

CN_{cell} is calculated according to eq. (11)

$$CN^{\mathrm{A}}_{\mathrm{cell}} = \sum_{\mathbf{T}=-\mathbf{T}_m}^{\mathbf{T}_m} \sum_{B}^{N}{}' \left[1 + e^{-k_1\left(k_2 \frac{R_{\mathrm{A,cov}}+R_{\mathrm{B,cov}}}{R_{\mathrm{AB}}}-1\right)}\right]^{-1} \cdot CN_{\mathrm{damp}}(R_{\mathrm{AB}}) \quad (11)$$

With these modifications the fractional CN^{A} and therewith the C_6-parameter and $E^{\mathrm{cell}}_{\mathrm{D3}}$ converge well with t^{max} (see Figs. 1 and 2). For graphite, calculations with $t^{\mathrm{max}} = 8$ and $t^{\mathrm{max}} = 30$ result in the same lattice parameter c, see Figure 3.

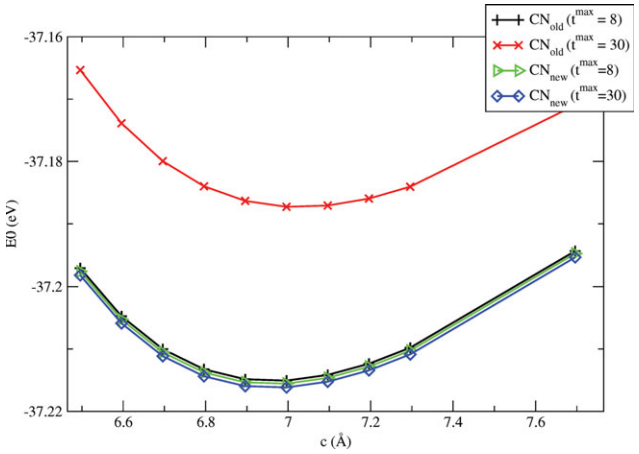

Figure 3. Graphite: Potential curves for lattice parameter c for $t^{\mathrm{max}} = 8$ and $t^{\mathrm{max}} = 30$. CN_{old} according to eq. (3), CN_{new} according to eq. (10). [Color figure can be viewed in the online issue, which is available at wileyonlinelibrary.com.]

For the D2 correction we compared results obtained with our implementation with results with the original VASP code for selected systems. Both versions produce–within a few meV–the same dispersion correction energy. The small differences can be ascribed to the different cutoff criteria.

Convergence tests

In our implementation, the dispersion correction for the calculated supercell depends on the chosen values for t_a, t_b, and t_c. These must be large enough to ensure that the dispersion energy term is converged. But although its calculation is not expensive, the summation in eq. (6) and (7) may become quite cumbersome for large supercells. Therefore, we checked the convergence behavior in preliminary calculations on simple systems. $E^{(3)}$ terms were not calculated for this check. We chose the Cu bulk with the primitive unit cell containing one atom and the benzene adsorption on the Ag(111) surface with a supercell containing 72 atoms (60 Ag Atoms). For the Cu bulk, we find convergence for $t^{\mathrm{max}} = 8$, see Figure 4, and for the benzene adsorption on Ag(111) convergence is already reached for $t^{\mathrm{max}} = 4$.

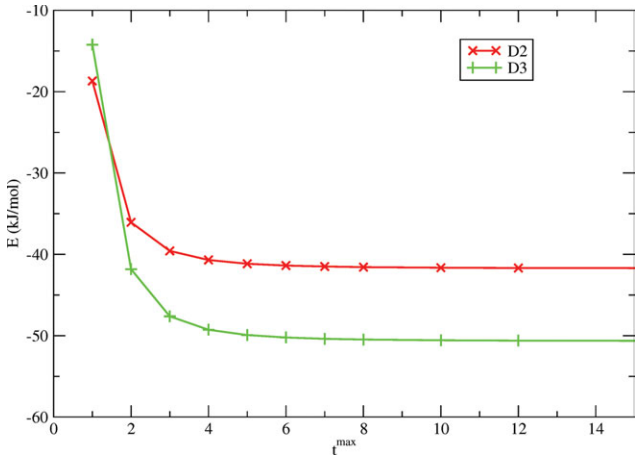

Figure 4. Convergence test for the Cu bulk: E_{D2} and E_{D3} are plotted against t^{max}. [Color figure can be viewed in the online issue, which is available at wileyonlinelibrary.com.]

Methodology

All calculations were performed with the plane-wave code VASP in combination with the projector-augmented wave method to account for the core electrons.[30–33] A relatively high cutoff energy of 600 eV for the plane-wave valence basis was used for the calculations of the bulk systems. This value was reduced to 400 eV for adsorption of benzene and Xe on the Ag(111) surface for computational reasons. The chosen Monkhorst-Pack integration setup depends on the system. As example, we used a 21 × 21 × 21 k-point mesh for Cu, Ag, Au and graphite, a 4 × 4 × 4 k-point mesh for the molecular crystals benzene, urea and formamide, and a 3 × 3 × 1 k-point mesh for the adsorption on the Ag(111) surface using a supercell. The chosen values are a compromise between accuracy and computational efficiency.

We applied the Perdew-Burke-Ernzerhof (PBE) functional because it is widely used in quantum solid-state chemistry and because PBE-D2 and PBE-D3 have been successfully used in our previous studies of formamide adsorption on Ag(111)[29] and the interactions within the formamide bulk.[34] We used the D3 implementation without the $E^{(3)}$ terms except where noted otherwise. Calculations where $E^{(3)}$ terms are considered are denoted as PBE-D3(ABC). Their results are discussed in a separate section Influence of Three-Body Terms. As gradients for the cell relaxation are not yet implemented in the dispersion correction code we perform the optimizations of the lattice parameters numerically. Due to restrictions of computer resources we did not calculate the zero-point and thermal corrections to the cohesive and adsorption energies.

Metals and metal oxides

Our first test set consists of the coinage metals copper, silver, and gold. Their crystal structures belong to cubic space group *Fm3m*. The calculated lattice parameters and cohesive energies are summarized in Table 1. Standard PBE gives only a small deviation of +0.6% for the Cu lattice parameter a. The overestimation of a increases to about 2% for Ag and Au. PBE-D2 does not show a well-defined trend. The lattice parameter a is underestimated by about 1.5% for Cu and Au, whereas it is still overestimated for Ag because there is almost no change

Table 1. Comparison of calculated and measured bulk properties of crystalline copper, silver, and gold (space group *Fm*3*m*); lattice parameter *a* in Å, relative deviation Δa from experimental values[35] in percentage, cohesive energy E_{coh}, total deviation from experimental values[35] ΔE_{coh} in kJ/mol.

	PBE				PBE-D2				PBE-D3			
	a	Δa	E_{coh}	ΔE_{coh}	*a*	Δa	E_{coh}	ΔE_{coh}	*a*	Δa	E_{coh}	ΔE_{coh}
Cu	3.636	+0.6	335	−2	3.572	−1.2	376	+39	3.569	−1.3	385	+48
Ag	4.165	+1.9	240	−45	4.157	+1.7	295	+10	4.090	+0.1	287	+2
Au	4.173	+2.3	288	−78	4.014	−1.7	429	+63	4.115	+0.7	351	−15

compared with PBE. One reason for this behavior might be that the D2-correction is not explicitly parameterized for each *d*-element. Applying the D3 correction the lattice parameter *a* is reduced by 0.06–0.07 Å with respect to PBE for all three elements. This results in an underestimation of *a* for Cu by 1.3%, a nearly perfect agreement for Ag and an overestimation by 0.7% for Au. The D3 correction gives considerably better results for Ag and Au, whereas it leads to a deterioration for Cu whose lattice parameter is already well described with PBE.

The calculated cohesion energies E_{coh} (see Table 1) reflect the results for the lattice parameters. PBE gives a good agreement with experimental results for copper, whereas E_{coh} is largely underestimated, by 45 kJ/mol for Ag and by 78 kJ/mol for Au. In contrast PBE-D3 shows only small deviations of +2 kJ/mol for Ag and of −15 kJ/mol for Au but a larger deviation of +48 kJ/mol for Cu. The D3 correction increases the cohesion energy by an almost constant energy value ranging from 50 to 60 kJ/mol. Again, no clear trend for the PBE-D2 functional was observed.

The second test set consists of the binary oxides MgO (space group $Fm\bar{3}m$), Al_2O_3 (corundum, space group $R\bar{3}c$), and TiO_2 in both the rutile ($P4_2/mnm$) and the anatase ($I4_1/amd$) polymorphs. As shown in Table 2 standard PBE works quite well for these systems which was expected because the oxides are to a large extend ionic and have a relatively small polarizability. Dispersion effects should therefore be small. The deviation from experimental results is in the range of 1% for most lattice parameters. The only exception is lattice parameter *c* for anatase with a deviation of +2.2%. In these cases PBE-D2 and PBE-D3 give results similar to each other. Most lattice parameters are decreased by 0.03–0.10% compared to PBE. But overall the PBE-D3 functional gives the best results. Its maximum deviation is 1.1% and it is the only method which gives a satisfactory result for the *c* lattice parameter of anatase.

In the next test set, we consider the layer compounds V_2O_5, MoS_2, and graphite, see Table 3. In these compounds, the weak interaction between the layers is dominated by dispersion. Not surprisingly, the standard PBE functional fails for these systems. The lattice parameter *c* that describes the interlayer distance is overestimated by about 11% for vanadium pentoxide and by approximately 30% for molybdenum disulfide and graphite. This difference can be understood by the fact that the graphite and MoS_2 layers are only held together by dispersion interaction between the carbon and sulfur atoms, respectively, whereas additional dipole-dipole interactions play a role for V_2O_5. In our optimization, the other lattice parameters of MoS_2 and graphite were fixed to their experimental values to circumvent problems with numerical stability of the numerical optimization with PBE.

As expected, the PBE-D2 and PBE-D3 functionals represent a considerable improvement for the interlayer parameters: The attractive interlayer binding of graphite and MoS_2 is correctly described, and the deviation for V_2O_5 is reduced to 2.4% (PBE-D2) and 0.8% (PBE-D3), respectively. However, both approaches have problems with graphite. The D2-correction underestimates the lattice parameter *c* by about 4%, whereas the D3-correction overestimates it by about 3%. In all cases, the cohesive energies are severely overestimated by the DFT-D methods. This is due to the counterintuitive overbinding of the underlying PBE method of 290 kJ/mol (V_2O_5) and 50 kJ/mol (graphite). Only for MoS_2 the PBE error ΔE_{coh} is negative, −35 kJ/mol.

Molecular crystals

The last bulk test set consists of molecular crystals of benzene, formamide, and urea. These systems were chosen as they represent some of the most important intermolecular interactions: The benzene bulk is mainly held together by dispersion

Table 2. Comparison of calculated and measured bulk properties of crystalline MgO, Al_2O_3, and TiO_2 (anatase and rutile); lattice parameters *l* in Å, relative deviation Δl from experimental values[36] in percentage, cohesive energy E_{coh}, total deviation from experimental values[35] ΔE_{coh} in kJ/mol.

	PBE				PBE-D2				PBE-D3				exp.	
	l	Δl	E_{coh}	ΔE_{coh}	*l*	Δl	E_{coh}	ΔE_{coh}	*l*	Δl	E_{coh}	ΔE_{coh}	*l*	E_{coh}
MgO														
A	4.24	+0.5	1004	+1	4.19	−0.7	1059	+56	4.20	−0.4	1044	+41	4.22	1003
Al_2O_3														
A	4.81	+1.1	3129	+46	4.79	+0.6	3244	+161	4.79	+0.6	3204	+121	4.760	3083
C	13.13	+1.0			13.03	+0.3			13.06	+0.5			12.99	
TiO_2:Rutile														
A	4.66	−0.6	1961	+46	4.62	−1.5	2015	+100	4.65	+1.3	2013	+102	4.59	1915
C	2.97	0.0			2.98	+0.3			2.96	−0.3			2.97	
TiO_2:Anatase														
a	3.82	+1.1	1969	+59	3.80	+0.5	2012	+102	3.82	+1.1	2017	+117	3.78	1910
c	9.71	+2.2			9.73	+2.4			9.58	+0.8			9.50	

Table 3. Comparison of calculated and measured bulk properties of crystalline V_2O_5, MoS_2 and graphite; lattice parameters l in Å; relative deviation Δl from experimental values[36] in percentage, cohesive energy E_{coh}, deviation from experimental values[35] ΔE_{coh} in kJ/mol.

	PBE				PBE-D2				PBE-D3				exp.	
	l	Δl	E_{coh}	ΔE	l	Δl	E_{coh}	ΔE	l	Δl	E_{coh}	ΔE	l	E_{coh}
V_2O_5														
A	11.56	+0.3	4115	+290	11.63	+1.0	4200	+375	11.65	+1.1	4190	+365	11.519	3825
B	3.56	0.0			3.53	−1.0			3.55	−0.4			3.564	
C	4.85	+10.9			4.48	+2.4			4.41	+0.8			4.373	
MoS_2														
a	—[a]	—	∼1414	−35	3.19	+1.2	1565	+117	3.16	+0.3	1565	+117	3.15	1448
c	∼14.9	∼30			12.42	+1.0			12.34	+0.3			12.30	
Graphite														
c	∼8.8	∼30	∼768	+50	6.432	−3.9	779	+62	6.906	+3.1	777	+60	6.69	717

[a] Not optimized.

interaction, the urea bulk by an extended three-dimensional hydrogen bond network, and the formamide bulk by a two-dimensional amide hydrogen bond network within the (101) layers and by dispersion and C—H ··· O hydrogen bonds between the (101) layers.[34] The results are summarized in Table 4,5, and 6. As expected, PBE does not accurately describe the benzene bulk structure. The lattice parameters are overestimated by up to 14%. In contrast, PBE-D2 gives parameters which are too short by more than 2.5%. Only PBE-D3 gives satisfactory results with a maximum deviation of 1.2%. PBE-D3 also shows (with a deviation of only 0.1%) the best performance for the urea bulk, whereas PBE results in too long and PBE-D2 in too short parameters. Also the bulk structure of formamide is not correctly described with PBE. A much too large value of 4.65 Å (not shown in Table 6) is obtained for lattice parameter *a* (exp. value: 3.54 Å). This can be explained by the fact that the forces along the *a* direction are dominated by dispersion interaction and weak C—H ··· O hydrogen bonds. Both, PBE-D2 and PBE-D3, give a reasonable agreement with experimental results. PBE-D3 gives smaller deviations for the lattice parameters *b* and *c* within the (101) layer, but overestimates the *a* parameter by 2.1%.

Table 4. Comparison of calculated and measured bulk properties of benzene; lattice parameters *a,b,c* in Å, relative deviation from experimental values[37] in percentage, heat of sublimation H_{sub}, deviation from experimental values[36] in kJ/mol.

	PBE		PBE-D2		PBE-D3		exp.
a	7.981	+8.5	7.169	−2.6	7.418	+0.8	7.357
b	10.194	+8.8	9.102	−2.9	9.353	−0.2	9.373
c	7.667	+14.4	6.482	−3.3	6.780	+1.2	6.701
H_{sub}	11	−31	56	+15	57	+16	41

Table 5. Comparison of calculated and measured bulk properties of urea; lattice parameters *a,c* in Å, relative deviation from experimental values[38] in percentage, heat of sublimation H_{sub}, deviation from experimental values[36] in kJ/mol.

	PBE		PBE-D2		PBE-D3		exp.
a	5.804	+4.3	5.461	−1.9	5.558	−0.1	5.565
c	4.704	+0.4	4.652	−0.7	4.681	−0.1	4.685
H_{sub}	82	−21	116	+13	117	+14	103

Table 6. Comparison of calculated and measured bulk properties of formamide; lattice parameters *a,b,c,β* in Å and degrees, relative deviation from experimental values[39,40] in percentage, heat of sublimation H_{sub}, deviation from experimental values[36] in kJ/mol.

	PBE-D2		PBE-D3		exp.
a	3.514	−0.8	3.617	+2.1	3.543
b	8.850	−1.1	8.995	+0.5	8.951
c	6.979	+0.1	6.952	−0.3	6.974
β	101.8	+0.7	100.0	−1.1	101.1
H_{sub}	85	+18	87	+20	67

Adsorption on surfaces

Finally, we examined the adsorption of Xe and benzene on the Ag(111) surface as benchmarks for the adsorption on metal surfaces. These systems have been subjected to numerous theoretical studies.[41–43] For both systems, the adsorbate-surface binding consists predominantly of dispersion interactions. For the benzene adsorption, we studied the adsorption on a threefold-hollow site with both $C_{3v}(\sigma_v)$ and $C_{3v}(\sigma_d)$ symmetry and an on-top position for Xe. Figures 5 and 6 show potential curves for both adsorption sites. The PBE description of the benzene and the Xe adsorption leads to potential curves with extremely flat minima of about −5 kJ/mol (benzene) and −2 kJ/mol (Xe), respectively. In both cases, we get a much too large distance to the surface of about 3.8 Å for benzene and of about 4.2 Å for Xe.

PBE-D2 and PBE-D3 give considerably improved the agreement with available experimental data. For benzene, PBE-D2 gives a minimum at a distance of 2.95 Å and an adsorption energy of −90 kJ/mol. The PBE-D3 minimum lies at 3.15 Å and corresponds to an adsorption energy of −71 kJ/mol. Both methods overestimate the absolute value of the experimental adsorption energy (−51 kJ/mol) for the $C_{3v}(\sigma_v)$ configuration.[44] However, the deviation with the PBE-D3 functional is considerably smaller than with PBE-D2. Again one has to keep in mind, that the zero point energy and thermal corrections, that are expected to lower the adsorption energy, are not considered. In agreement with experiment, we find that the $C_{3v}(\sigma_d)$ configuration is more stable than $C_{3v}(\sigma_v)$. To the best of our knowledge, no experimental data for the benzene-Ag distance are available until now. For the Xe adsorption PBE-D2 and PBE-D3 give similar results. The adsorption energy is −27 kJ/mol (PBE-D2) and −26

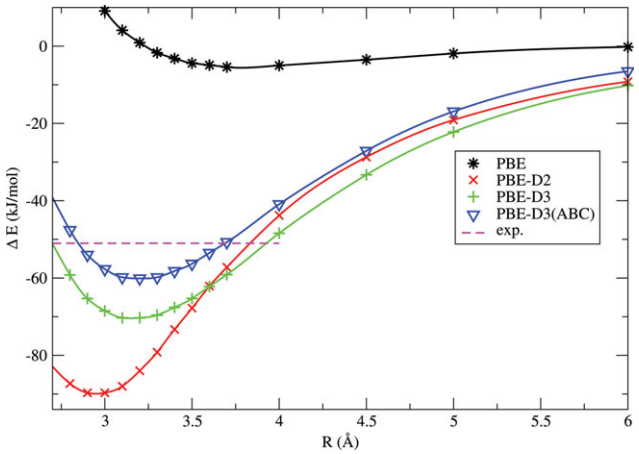

Figure 5. Potential curves [PBE, PBE-D2, PBE-D3, and PBE-D3(ABC)] for the adsorption of benzene on the Ag(111) surface.

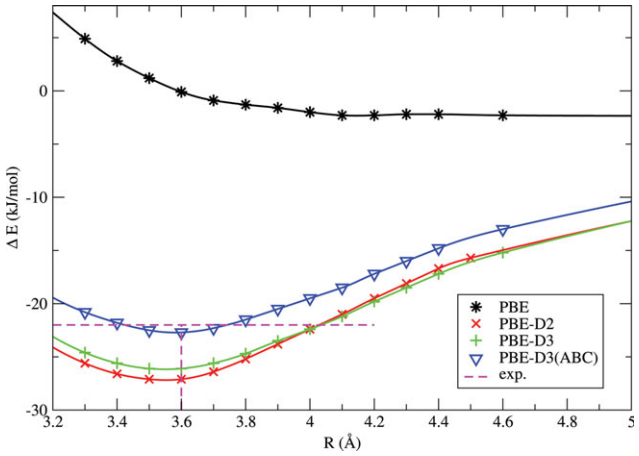

Figure 6. Potential curve [PBE, PBE-D2, PBE-D3, and PBE-D3(ABC)] for the adsorption of Xe on the Ag(111) surface.

kJ/mol (PBE-D3), and the distance to the surface is 3.56 Å with both methods. These values are in good agreement with the experimental results of $R_{AgXe} = 3.6$ Å and $E_{ads} = -22$ kJ/mol.[45]

Influence of Three-Body Terms

The D3-correction takes into account the nonadditivity of dispersion interaction on the basis of the three-body terms E^{ABC}. As it was found that $E^{(3)}$ has only an insignificant contribution to E_{D3} for small and medium-sized molecules, their usage has not been recommended for such systems. However, their contribution was expected to grow for extended systems.[11]

To study the importance of nonadditive effects for solids and surfaces, we performed for all systems–with exception for the formamide bulk where convergence problems occurred–additional PBE-D3(ABC) calculations. The results are summarized in Table 7. As a general trend it was observed that $E_6^{(3)}$ is repulsive for all systems. The ratio $|E_6^{(3)}|/E_6^{(2)}$ is between 0.07 for V_2O_5 and 0.21 for Cu, thus the three-center contributions are not negligible. As consequence of the repulsive behavior

Table 7. Comparison of PBE-D3(ABC) results with PBE-D3 and experimental data; l is the PBE-D3(ABC) lattice parameter in Å, Δl is the relative deviation from the experimental value[35] in percentage, Δl (ABC) is the deviation from the PBE-D3 results in Å (left) and percentage (right), $\frac{E_6^{(3)}}{E_6^{(2)}}$ is the ratio between the three-center and two-center terms, E is the cohesive energy E_{coh} or heat of sublimation H_{sub} (urea and benzene), respectively, for PBE-D3(ABC) in kJ/mol, ΔE (ABC) (kJ/mol) is the change of E_{coh} or H_{sub} due to inclusion of three center terms.

System	l	Δl	Δl (ABC)		$\frac{E_6^{(3)}}{E_6^{(2)}}$	E	ΔE (ABC)
Cu							
a	3.592	−0.5	+0.02	+0.6	0.21	374	−11
Ag							
a	4.115	+0.6	+0.03	+0.6	0.18	278	−9
Au							
a	4.136	+1.6	+0.02	+0.5	0.18	336	−12
Al_2O_3							
a	4.80	+0.8	+0.01	+0.2	0.11	3191	−13
c	13.08	+0.7	+0.02	+0.2			
MgO							
a	4.21	−0.2	+0.01	+0.2	0.17	1036	−8
Rutile							
a	4.65	+1.2	0.00	0.0	0.14	2005	−8
c	2.96	−0.3	0.00	0.0			
Anatase							
a	3.83	+1.3	+0.01	+0.2	0.12	2013	−4
c	9.59	+0.9	+0.01	+0.1			
V_2O_5							
a	11.65	+1.1	0.00	0.0	0.07	3815	−10
b	3.56	0	+0.01	+0.3			
c	4.45	+1.8	+0.04	+0.9			
MoS_2							
a	3.17	+0.6	+0.01	+0.3	0.15	1553	−12
c	12.57	+2.2	+0.23	+1.8			
Graphite							
c	7.080	+5.8	+0.17	+2.5	0.14	775	−2
Urea							
a	5.58	+0.2	+0.02	+0.4	0.09	113	−4
b	4.68	−0.2	0.00	0.0			
Benzene							
a	7.48	+1.6	+0.06	+0.8	0.08	50	−7
b	9.46	+1.0	+0.11	+1.1			
c	6.86	+2.4	+0.08	+1.1			

PBE-D3(ABC) gives larger lattice parameters than standard PBE-D3. This effect is more pronounced for lattice parameters for which dispersion is important (e.g., parameter *c* for graphite, MoS_2 and V_2O_5, and all benzene lattice parameters), whereas it is less important for the strongly bound systems like Al_2O_3, MgO, and TiO_2. On the other hand, the effect of $E^{(3)}$ on cohesive energies and heats of sublimation are small, 2–13 kJ/mol which is negligible compared with other contributions such as the zero-point energy. The situation is different for adsorption studies. The PBE-D3(ABC) and PBE-D3 potential curves for the adsorption of benzene and Xe on the Ag(111) surface are compared in Figures 6 and 5. The three-body terms lead to an increase of the adsorbate-surface distance, to 3.20 Å for benzene and 3.59 Å for Xe. The adsorption energies decrease to −60 kJ/mol for benzene and −23 kJ/mol for Xe.

Our conclusion is that the E^{ABC} terms have a noticeable effect on distances and energies for solids and surface adsorption. We do not recommend PBE-D3(ABC) for solids, as most lattice parameters deteriorate compared with PBE-D3. This is particularly

the case for weakly bound systems like graphite, MoS_2, benzene, and V_2O_5. In addition, one has to keep in mind that the computational effort for the D3-correction strongly increases due to the $O(N^3)$ behavior of $E^{(3)}$. The benzene adsorption of Ag(111) is the only case where PBE-D3(ABC) gives considerably better results than PBE-D3. Therefore, the three-center terms are recommended for adsorption studies.

Summary and Conclusion

We implemented two empirical dispersion corrections into the plane wave-code VASP and tested their applicability to the calculation of solids and adsorption on surfaces. Results obtained with the more recent D3 correction are compared to D2 and corresponding standard PBE results. As expected a large improvement is obtained for all cases where standard DFT fails due to its insufficient description of dispersion. Both empirical PBE-D2 and PBE-D3 corrections give qualitatively and quantitatively correct results for the *c* parameter of the layer compounds graphite, MoS_2, and V_2O_5, for the *a* parameter of the formamide bulk, for the lattice parameters of the benzene bulk and for the adsorption of benzene and Xe on the Ag(111) surface. For oxides and metals which are already well described with standard PBE, we observe neither a general improvement nor deterioration. For example, best results for Cu and rutile are obtained with PBE, whereas the results for Ag, Au, Al_2O_3, anatase, and urea are best with PBE-D3. A comparison of the PBE-D2 and PBE-D3 results shows that PBE-D3 performs in almost all cases better than PBE-D2. Furthermore, we find no example where the PBE-D3 method completely fails. The consideration of three-body terms $E^{(3)}$ causes a slight increase of most lattice parameters due to their repulsive character. This leads to an overestimation of lattice parameter for weakly bound systems. As a result of this study we can recommend to use the D3 method as default for periodic calculations of bulk and surface properties. It is a computationally efficient method particularly well suited for the calculation of structural and energetic aspects of adsorption and structures of molecular crystals. In adsorption studies where dispersion plays a major role the inclusion of three-center terms should be considered.

Keywords: density functional theory · dispersion interaction · solids · surfaces

How to cite this article: W. Reckien, F. Janetzko, M. F. Peintinger, T. Bredow, *J. Comput. Chem.* **2012,** *33,* 2023–2031. DOI: 10.1002/jcc.23037

[1] R. Dronskowski, Computational Chemistry of Solid State Materials: A Guide for Materials Scientists, Chemists, Physicists and others; Wiley-VCH: Weinheim, **2005**.
[2] J. Kohanoff, Electronic Structure Calculations for Solids and Molecules—Theory and Computational Models; Cambridge University Press: Cambridge, UK, **2006**.
[3] Y. Zhao, N. E. Schultz, D. G. Truhlar, *J. Chem. Theor. Comp.* **2006**, *2,* 364.
[4] M. Dion, H. Rydberg, E. Schröder, D. C. Langreth, B. I. Lundqvist, *Phys. Rev. Lett.* **2004**, *92,* 246401.
[5] T. Thonhauser, V. R. Cooper, S. Li, A. Puzder, P. Hyldgaard, D. C. Langreth, *Phys. Rev. B* **2007**, *76,* 125112.
[6] O. A. Vydrov, T. V. Voorhis, *J. Chem. Phys.* **2010**, *133,* 244103.
[7] J. Harl, G. Kresse, *Phys. Rev. B* **2008**, *77,* 045136.
[8] M. Rohlfing, T. Bredow, *Phys. Rev. Lett.* **2008**, *101,* 266106.
[9] F. Ortmann, F. Bechstedt, W. G. Schmidt, *Phys. Rev. B* **2006**, *73,* 205101.
[10] A. Tkatchenko, L. Romaner, O. T. Hofman, E. Zojer, C. Ambrosch-Draxl, M. Scheffler, *MRS Bull.* **2010**, *35,* 435.
[11] S. Grimme, J. Antony, S. Ehrlich, H. Krieg, *J. Chem. Phys.* **2010**, *132,* 154104.
[12] S. Grimme, *J. Comput. Chem.* **2004**, *25,* 1463.
[13] S. Grimme, *J. Comput. Chem.* **2006**, *27,* 1787.
[14] S. Grimme, S. Ehrlich, L. Goerigk, *J. Comput. Chem.* **2011**, *32,* 1456.
[15] S. Ehrlich, J. Möllmann, W. Reckien, T. Bredow, S. Grimme, *Chem. Phys. Chem.* **2011**, *12,* 3414.
[16] S. Tosoni, J. Sauer, *Phys. Chem. Chem. Phys.* **2010**, *12,* 14330.
[17] S. Tosoni, A. D. Boese, J. Sauer, *J. Phys. Chem. C* **2011**, *115,* 24871.
[18] T. Kerber, M. Sierka, J. Sauer, *J. Comput. Chem.* **2008**, *29,* 2088.
[19] T. Bucko, J. Hafner, S. Lebegue, J. G. Angyan, *J. Phys. Chem. A* **2010**, *114,* 11814.
[20] G. M. Psofogiannakis, G. E. Froudakis, *J. Phys. Chem. C* **2009**, *113,* 14908.
[21] J. C. Conesa, *J. Phys. Chem. C* **2010**, *114,* 22718.
[22] K. Tonigold, A. Gross, *J. Chem. Phys.* **2010**, *132,* 224701.
[23] C. M. Zicovich-Wilson, B. Kirtman, B. Civalleri, A. Ramirez-Solis, *Phys. Chem. Chem. Phys.* **2010**, *12,* 3289.
[24] M.-T. Nguyen, C. A Pignedoli, D. Passerone, *Phys. Chem. Chem. Phys.* **2011**, *13,* 154.
[25] J. P. P. Ramalho, F. Illas, *Chem. Phys. Lett.* **2011**, *501,* 379.
[26] B. Civalleri, L. Maschio, P. Ugliengo, C. M. Zicovich-Wilson, *Phys. Chem. Chem. Phys.* **2010**, *12,* 6382.
[27] P. A. Garrain, D. Costa, P. Marcus, *J. Phys. Chem. C* **2011**, *115,* 719.
[28] G. Kresse, J. Furthmüller, *Comp. Mater. Sci.* **1996**, *6,* 15.
[29] W. Reckien, B. Kirchner, F. Janetzko, T. Bredow, *J. Phys. Chem. C* **2009**, *113,* 10541.
[30] G. Kresse, J. Hafner, *Phys. Rev. B* **1993**, *47,* 558.
[31] G. Kresse, J. Hafner, *Phys. Rev. B* **1994**, *49,* 14251.
[32] G. Kresse, J. Furtmüller, *Phys. Rev. B* **1996**, *54,* 11169.
[33] G. Kresse, D. Joubert, *Phys. Rev. B* **1999**, *59,* 1758.
[34] W. Reckien, T. Bredow, *Chem. Phys. Lett.* **2011**, *508,* 54.
[35] NIST Chemistry WebBook, http://webbook.nist.gov, **2009**, NIST Standard Reference Database Number 69, National Institute of Standards and Technology, Gaithersburg MD, 20899.
[36] D. R. Lide, CRC Handbook of Chemistry and Physics, 81st ed.; CRC Press: Boca Raton, FL, **2000**.
[37] G. A. Jeffrey, J. R. Ruble, R. K. McMullan, J. A. Pople, *Proc. R. Soc. Lond. A* **1987**, *414,* 47.
[38] S. Swaminathan, B. M. Craven, R. K. McMullan, *Angew. Chem.* **1984**, *B40,* 300.
[39] J. Ladell, B. Post, *Acta Cryst.* **1954**, *7,* 559.
[40] B. H. Torrie, C. O. Donovan, B. M. Powell, *Mol. Phys.* **1994**, *82,* 643.
[41] K. Toyoda, I. Hamada, S. Yanagisawa, Y. Morikawa, *J. Nanosci. Nanotechnol.* **2011**, *11,* 2836.
[42] R. Caputo, B. P. Prascher, V. Staemmler, P. S. Bagus, C. Wöll, *J. Phys. Chem. A* **2007**, *111,* 12778.
[43] A. Bilic, J. R. Reimer, N. S. Hush, R. C. Hoft, M. J. Ford, *J. Chem. Theor. Comp.* **2006**, *2,* 1093.
[44] T. J. Rockey, M. Yang, H. L. Dai, *J. Phys. Chem. B* **2006**, *110,* 19973.
[45] G. Vidali, G. Ihm, H.-Y. Kim, M. W. Cole, *Surf. Sci. Rep.* **1991**, *12,* 135.

Received: 6 March 2012
Revised: 8 May 2012
Accepted: 8 May 2012
Published online on 8 June 2012